https://doi.org/10.5194/angeo-2024-28
Preprint. Discussion started: 20 December 2024

Annales Geophysicae Discussions
Open Access

Small- and meso-scale field-aligned auroral current structures, their spatial and temporal characteristics deduced by Swarm constellation

Hermann Lühr [1*] and Yun-Liang Zhou [2]

1. GFZ German Research Centre for Geosciences, Section 2.3, Geomagnetism, Telegrafenberg, 14473 Potsdam, Germany

2. Department of Space Physics, Electronic Information School, Wuhan University, 430072 Wuhan, China

*Correspondence to: hluehr@gfz-potsdam.de

Abstract Magnetic field recordings by the Swarm A and C spacecraft during the Counter Rotation Orbit phase are used for checking the stationarity of auroral region small-and meso-scale field-aligned currents (FAC). The varying separation between the spacecraft in along- and cross-track direction during this constellation phase allow for determining the spatial and temporal correlation lengths for FAC structures of different along-track wavelengths. We make use of the cross-correlation analysis to check the agreement of the magnetic signatures at the two spacecraft. When the cross-correlation coefficient exceeds 0.75 at a time lag that equals the along-track time difference, the event is identified as stationary. It is found that meso-scale FACs of along-track wavelength >100 km are primarily stable for more than 40 s and over cross-track separations of 20 km. An important reason for their deselection is the latitudinal motion of the current system. Conversely, stable small-scale FACs (10-75 km wavelength) are found primarily only in a very limited space, up to about 12 km in cross-track and ~18 s in along-track time difference. This class of small-scale FACs is the typical one found commonly in the cusp region and near the midnight sector. Not all the FACs within this limited spatial and temporal regime are stable. In particular for those with high current density occurring during enhanced solar wind input we do not find equivalent signatures at the accompanying satellite. They seem to represent narrow solitary Alfvén wave features.

1. Introduction

Field-aligned currents (FAC) are commonly observed in magnetized plasmas due to the high electric conductivity along magnetic field lines. In near-Earth space they can be found in the ionosphere and magnetosphere, with particularly strong currents flowing within the auroral regions. FACs appear at a wide range of horizontal scales from less than a kilometer (e.g., Neubert and Christiansen, 2003; Rother et al., 2007) up to 1000 km (e.g., Iijima and Potemra, 1976; Anderson et al., 2014). Commonly, the observed current densities become larger the smaller the scales are. Pairs of upward and downward currents are mostly close together. Rother et al. (2007) reported strongest current densities for horizontal scales of about 1 km wavelength (including both current directions). Smaller scales are progressively damped at F-region altitudes (Lotko and Zhang, 2018).

Large-scale FACs at auroral latitudes can be treated as quasi-static circuits, having their source in the magnetosphere, and the closure current in the ionosphere acts as a dissipative load. For smaller scales of FACs, approaching 10s of km, the dynamic characteristics of the circuit become important, and reflection at the ionosphere play a role (e.g. Lysak, 1990; Vogt and Haerendel,

https://doi.org/10.5194/angeo-2024-28
Preprint. Discussion started: 20 December 2024

Annales Geophysicae
Discussions

1998). Thus, Alfvén waves, carried by FACs, are becoming the dominate feature in the kilometer-scale range. Ishii et al. (1992) made use of magnetic and electric field measurements by the Dynamic Explorer 2 satellite for distinguishing between waves and static current circuits. From the amplitude relation between the two fields, they could discriminate the two types of FAC observations, showing that a cutoff exists for stationary FACs exists at the small-periods end around 4 s to 10 s. When considering the satellite velocity of about 7.5 km/s, the apparent periods convert to latitudinal wavelengths of 30 km to 75 km.

When deriving FAC estimates from satellites, one important assumption is the stationary of the magnetic signal over the time of measurement. This is not always satisfied. As reported by Stasiewicz et al. (2000) in their review article, small-scale FAC structures are commonly associated with kinetic Alfvén waves. Therefore, the current strength exhibits a significant temporal variation. From single-satellite magnetic field measurements it is not possible to distinguish between temporal and spatial variations. To overcome this problem Gjerloev et al. (2011) made use of the three ST5 satellites in pearls-on-a-string formation. They performed a large statistical study of the FAC temporal stability depending on their along-track scale size. On the nightside FAC structures larger than 100 km had been found to be quasi-stationary, while on the dayside this was only true for scales above 200 km. Due to their orbital geometry, the ST5 spacecraft were cycling the Earth in a sun-synchronous mode, which provided only little local time coverage. Furthermore, the orbits of the three spacecraft were well lined up. Therefore, no information on the longitudinal correlation length of FAC structures could be achieved. A similar study of FAC spatial and temporal scales was performed by Lühr et al. (2015), making use of the three Swarm spacecraft soon after launch when the satellites where slowly separating from each other. These authors generally confirmed the results of Gjerloev et al. (2011). FACs of scales up to some 10s of kilometer are highly variable with typical persistent periods of about 10 s. Larger-scale FACs (>150 km) can be regarded as quasi-stationary, being stable over more than 60 s. Concerning the longitudinal extension of the small FAC sheets, it was found to be 4 times large than the latitudinal width on the nightside, but on the dayside both scales were found to be comparable. In spite of these valuable results, that study had a number of limitations. The data were taken during December 2013 - January 2014, over less than 50 days. Thereafter, dedicated orbit maneuvers were performed. This means, it was not possible to investigate any seasonal dependences nor get a good local time coverage.

One of the standard Swarm Level-2 data products is the FAC density estimate derived from the magnetic field measurements of the Swarm A and Swarm C spacecraft flying side-by-side. An important assumption for the reliability of the product is that both satellites record magnetic field variation caused by the same FAC structure. In a dedicated study Forsyth et al. (2017) compared the recordings at the two Swarm spacecraft by means of a cross-correlation analysis. They generally find large cross-correlation coefficients when the magnetic field data are low-pass filtered with a cutoff of about 20 s. In addition, these authors request a similarity in signal amplitude at the two satellites, not exceeding a difference of 10%. This request significantly reduces the number of suitable data pairs for FAC estimates. We do not consider the amplitude request as justified because the FAC estimate derived from the dual-spacecraft approach is the mean value of the estimates at the two sites, and therefore the dominating linear part of the spatial, temporal gradient is taken care of by the averaging.

What is missing after all these studies is a detailed investigation of the smaller-scale FACs. What are their spatial, temporal correlation lengths? This information is needed, e.g., for determining the range dual-spacecraft FAC estimates. An opportunity for this kind FAC scale-size analysis erose during the Swarm Counter-Rotating Orbit Phase in 2021. During that campaign the orbits of Swarm A and C were brought close together, and Swarm B cycled the Earth in opposite direction. Early October 2021 all three orbital planes were quasi-coplanar. Thereafter, the orbits slowly separated again. For the study presented here we make use of the magnetic field recordings from

https://doi.org/10.5194/angeo-2024-28
Preprint. Discussion started: 20 December 2024

Annales Geophysicae Discussions Open Access EGU

1 May 2021 to 28 February 2022. The dataset covers both June and December solstices and for both seasons all local times are visited. We make use of the cross-correlation analysis, which is applied to the transverse magnetic field component of the Swarm A and C satellites. As a result, we obtain the variation of cross-correlation coefficient and its dependence on the spacecraft separations in along- and cross-track directions. This allows us to address a number of remaining questions concerning the temporal and spatial scales of small- and meso-scale FAC structures.

In the section to follow we present the Swarm mission and magnetic field data, in addition, the preprocessing is described. Section 3 introduces the cross-correlation analysis, our prime tool for determining the similarity between the magnetic field signatures at the two spacecraft. This is followed by a statistical analysis, in Section 4, of the derived correlation results during the 10 months of our study period. It includes both the characteristics of the identified stable and unstable FAC events separately for 6 spatial scale ranges. The obtained results are discussed in Section 5. Here we try to explain the behavior of the current structures and compare the findings with earlier publications. The Summary and Conclusions give a wrap-up of the derived auroral zone FAC stability characteristics.

2. Data and processing approach

ESA's Swarm satellite mission was launched on 22 November 2013. It comprises three identical satellites in near-polar orbits at different altitudes (Friis-Christensen et al., 2008). During the first mission phase, starting on 17 April 2014, the lower pair, Swarm A and C, was flying at an altitude of about 450 km side-by-side with a longitudinal separation of 1.4°, while the third, Swarm B, cruised about 60 km higher. Due to their orbital inclination of 87.3°, Swarm A/C need about 133 days to cover all 24 local time (LT) hours, when considering both ascending and descending orbital arcs. Swarm B, with a slightly larger inclination (88°) needs about 141 days for a full local time coverage. As a consequence of the difference in inclination, the angle between the orbital planes of Swarm A/C and Swarm B slowly increased.

In preparation for a second mission phase, the counter-rotating orbits campaign, the longitudinal separation between Swarm A and C was slowly reduced starting in October 2019. Around 1 October 2021 the orbital planes of Swarm A/C and Swarm B were quasi coplanar. All three crossed the equator at similar longitudes, with Swarm B flying in opposite direction (e.g., Xiong and Lühr, 2023). Thereafter, the separation between Swarm A and C orbital planes increased again at a rate of 0.7° in longitude per year. The months of small Swarm A/C separation around the epoch of coplanarity are of special interest for this study.

Here we make use of the Swarm Level-1b 1 Hz magnetic field data with product identifier "MAGx_LR", where lower-case "x" in the product names represents a placeholder for the spacecraft, A, B, C. The magnetic vector data are given in the North-East-Center (NEC) frame. For our purpose we remove from the Swarm A and C magnetic field observations the contributions of core, crustal, and magnetospheric fields by subtracting the geomagnetic field model CHAOS-7.11 (Finlay et al., 2020). The residuals of the horizontal components, Bx and By, are used for studying the magnetic signatures caused by the FACs. From these two components we calculate the deflections of, B_{trans}, transverse to the flight direction.

$$B_{trans} = B_y\, cos(\gamma) - B_x\, sin(\gamma) \qquad (1)$$

where $sin(\gamma) = cos(incl)/cos(lat)$ with $incl$ as orbital inclination and lat as latitude of measurement point. For application in Eq. (1) $\gamma = \gamma$ has to be used on the ascending part of the orbit and $\gamma = \pi - \gamma$ on the descending part.

https://doi.org/10.5194/angeo-2024-28
Preprint. Discussion started: 20 December 2024

Annales Geophysicae
Discussions

We actually used in our further investigations the difference between two adjacent values of B_{trans}, separated by 1 s. These differences, ΔB_{trans}, help to remove remaining large-scale biases after model subtraction; furthermore, they better represent the characteristics of FACs. A related single-satellite FAC estimate would read

$$j_z = \frac{1}{\mu_0}\frac{\Delta B_{trans}}{v_{SC}} \quad (2)$$

where μ_0 is the vacuum permeability and v_{SC} is the spacecraft velocity. When inserting, for example, ΔB_{trans} = 10 nT/s and the typical orbital speed of Swarm, 7.55 km/s, we obtain for the FAC density, $j_z = 1.1$ µA/m^2. This means, the FAC intensities amount approximately to a tenth of the B-field change rate.

Several phenomena are associated with FACs of different scale sizes. In order to identify these FAC properties we subdivide the signal of ΔB_{trans} into six quasi-logarithmically spaced period bands. The chosen -3 dB pass-band filter limits are 1-3 s, 3-7 s, 7-13 s, 13-23 s, 23-39 s, and 39-60 s.

The studied interval lasts from 1 May 2021 to 28 February 2022. During these months the Swarm A/C cross-track separation is small and stays below 20 km at auroral latitudes. The along-track separation between the spacecraft is deliberately modified around the time of coplanarity between 2 s and 41 s, as shown in Figure 1 of Zhou et al. (2024). The same figure displays also the variation of longitudinal (cross-track) separation at the equator over the study period. Here we are interested in the small and meso-scale FAC characteristics at auroral latitudes beyond ±60° magnetic latitude (MLat).

3. Correlation analysis

A common assumption, when estimating FAC density from magnetic field satellite observations, is that the signal is quasi-stationary. This condition can be tested, when Swarm A and C observe the same current structure. We check the stationarity with the help of a cross-correlation analysis.

$$Cc = \frac{\sum[(X-X_m)\cdot(Y-Y_m)]}{\sqrt{\sum(X-X_m)^2\cdot\sum(Y-Y_m)^2}} \quad (3)$$

where, X represents the signal amplitude of ΔB_{trans} from Swarm A, Y represents the signal of ΔB_{trans} from Swarm C, and Xm and Ym represent the mean values of ΔB_{trans} over the correlation intervals of the two satellites, respectively. We further determine the maxima of Cc and the corresponding time lags (T-lag) between the two satellite data series. It has to be noted that in this way T-lag is derived only with a one-second resolution, as the Swarm magnetic measurements have a 1-s resolution. For improving this situation, we consider the five cross-correlation results centered on the maximum Cc value and apply a fourth-order polynomial fitting. From the peak location of the fitted polynomial, we get the T-lag in fractions of a second. According to the definition of Cc in Eq. (3), a positive T-lag means, Swarm A samples the magnetic signal before Swarm C.

Figure 1 presents examples of passes over the north pole. The upper frame is from 1 September 2021, along a midnight - noon orbit. For these example-passes we consider an interval of 60 s (corresponding to a distance of 450 km) of ΔB_{trans} from Swarm A and C to calculate the root mean square (RMS) amplitude and to perform the cross-correlation analysis. The ΔB_{trans} in the top panel shows two groups of signal bursts at auroral latitudes in the recordings of the two satellites. These represent intense FAC at a wide range of scales, the earlier one occurring around midnight and the other at noon. For getting an impression of the related FAC densities, a ΔB_{trans} amplitude of 100

https://doi.org/10.5194/angeo-2024-28
Preprint. Discussion started: 20 December 2024

Annales Geophysicae Discussions

nT/s corresponds, as shown above, to approximately 10 μA/m^2. The RMS values are given in the second panel. In the third panel optimal T-lag values are plotted. Over large parts of the pass it stays close to the actual time shift, Δt = 4 s, between the spacecraft, as expected for a static structure. The *C*c values at the bottom herald good correlation (*C*c > 0.75) for most of the signal. However, that is not always the case for the bursts. In this example, the equatorward part of the nightside burst exhibits an almost perfect correlation at expected lag time, while the correlation on the poleward side is poor. At noon the cross-correlation coefficient is also below the threshold on the poleward parts but is high during the stronger later burst.

In the lower frame of Figure 1 an example from 1 January 2022 is displayed. The recordings, in the same format as above, are again from a noon - midnight pass. Bursts of small-scale FACs appear around 78° MLat. An obvious difference to the example shown above is the generally low cross-correlation coefficient. Here again, the more equatorward parts of the bursts tend to show larger *C*c. The major difference of this example compared to the former is the much longer along-track separation between the two satellites of Δt = 22.3 s. In spite of that enlarged distance, best correlation between the two recordings is achieved at time lags close to the actual time difference, but the quality of correlation has decreased considerably.

These examples show that small-scale FACs do reach large amplitudes at auroral latitudes, but they cannot generally be considered as static structures.

4. Statistical analysis

The aim of our study is to identify the typical properties of small- and meso-scale FAC structures at auroral latitudes. Such information can best be achieved when simultaneous observations from multiple points are available. For the statistical analysis we considered the time 1 May 2021 - 28 February 2022, when the orbital planes of Swarm A and C differed only by small angle (<0.3°). This promises meaningful multipoint measurements down to the smallest resolvable scales of <10 km.

The study interval overlaps with the trailing part of the solar minimum. Therefore, the mean solar flux level increases slowly from F10.7 = 80 sfu in the beginning to about F10.7 = 110 sfu around the end. The magnetic activity stays generally below Kp = 4. There were just some stormy days, quite outstanding is 4 November 2021, followed at decreasing activity levels by 12 October 2021 and 4 February 2022. Due to the generally calm conditions, the derived mean FAC characteristics represent normal solar wind driving states.

It is known from earlier publications that FACs of different scales exhibit different dynamic properties, e.g. Stasiewicz, K., et al. (2000) and references therein. For that reason, we divided the magnetic variations ΔB_{trans} into the six period bands as outlined in Section 2. The cross-correlation analysis, as defined in Eq. (3), was applied separately to all the period bands and all the days. A current structure is considered as stationary when the magnetic field measurements from the two Swarm spacecraft achieve a peak cross-correlation coefficient, *C*c > 0.75, at a time shift that fits the along-track separation, Δt ±1.5 s. In order to avoid fault results from too small signals, in addition a minimum RMS amplitude is requested. For the decision on a suitable threshold, we considered the following facts. In their study on low-latitude FAC properties Zhou et al. (2024) had chosen a rather small amplitude limit, RMS > 0.03 nT/s. As can be seen from their Figure 2, FAC signatures frequently surpass 1 nT/s. Those FACs are generally driven by atmospheric processes, as winds and waves. Here we are interested in FACs driven by magnetospheric processes, therefore those from atmospheric dynamics, also active at auroral latitudes, should be suppressed. For that reason, we decided to choose a threshold, RMS > 2 nT/s, in this study. For assessing the consequence of this selection, Figure 2 shows the occurrence distribution of wavy magnetic signals at auroral latitudes beyond 60° MLat and within the period range of 1-60 s

https://doi.org/10.5194/angeo-2024-28
Preprint. Discussion started: 20 December 2024

(corresponding to wavelengths up to 450 km). As expected, the occurrence rate declines, the larger the threshold. For RMS > 2 nT/s about 60% of the satellite recordings provide significant FAC signal. This percentage fits also approximately the typical latitude range of Iijima and Potemra (1976) FAC coverage of the auroral oval.

4.1 Variation of identified static structures over the study period

Here we start with a look at the wavy magnetic field signal that could be caused by FACs and how this activity varies over the cause of our study period. Figure 3 presents the occurrence frequency, on a daily base, of wavy signals with amplitudes RMS > 2 nT/s, as recorded by Swarm A, separately for the six period ranges and the two hemispheres. No comparison with Swarm C measurements has been performed. Across the bottom of the figure additional information is added, the typical orbital local time (taken at 70° MLat) separately for up- and downleg arcs, the along-track time difference between Swarm A and C, and the east-west separation of the spacecraft at the equator in degree.

The curves for the different periods are quite similar. They reach up to rates of 50%. This is expected as a result of our chosen RMS threshold. General features to be noticed; higher rates are observed at local summer conditions. This is the case during the first half of the study period in the northern hemisphere and the second half in the southern. More events are found during daytime than at night. This holds for both hemisphere but is more pronounced for shorter periods (smaller structures) and for local summer time. The occurrence rate varies partly at regular period. This is close to 13.5 days, reflecting halve the rotation period of the sun. There appears a particularly deep dip in occurrence rate at 27-28 October 2021. This is a time of very low magnetic activity, having obviously direct influence on the FAC activity at auroral latitudes. Only one week later, 3-4 November, a major magnetic storm occurred, giving rise to enhanced signal rates, in particular, in the southern hemisphere.

For comparison, Figure 4 shows for the two hemispheres the temporal variation of the mean occurrence rates of positively detected static structures by means of cross-correlation between Swarm A and C recordings, separately for the up- and downleg orbital arcs within auroral latitudes (beyond 60° MLat), in the same format as before. Particularly low event occurrences are found at the smallest scales (1-3 s). Only during the 2 weeks around coplanarity (1 October) somewhat enhanced rates appear. Within that fortnight the along-track separation was reduced to Δt = 2 s. This indicates rather small correlation length of these narrow FACs. For larger current structures the curves start to agree more and more with the before shown activity curves, at least for the first half of the study period. During the second half we find a prominent dip in event occurrences centered on December 2021. In that month the along-track separation is particularly large between Swarm A and C.

Finally, Figure 5 presents the ratio of magnetic signatures that can be interpreted as stable FAC structures. Plotted are the daily detected static structures divided by the counts of activity intervals. These normalized curves reveal which fraction of the high latitudes is covered by stable FACs of different scale-lengths. Rather similar curves are derived from the two hemispheres. Towards longer periods (larger scales) fairly constant ratios between 80% and 100% are derived. This confirms that almost all FACs of these scales at auroral latitudes can be considered as quasi stationary. The rates start to drop for shorter periods shorter than ~10 s (<75 km along-track). Particularly low percentages are returned for the very short period (1-3 s). Also here, the rates are somewhat outstanding in the 2 weeks around orbit coplanarity, when the spacecraft separation was reduced to 2 s. Peak occurrence ratios can also be found for other period bands during those two weeks.

https://doi.org/10.5194/angeo-2024-28
Preprint. Discussion started: 20 December 2024

Annales Geophysicae Discussions

When normalizing the identified FAC structures by the number of wavy signal events above a certain amplitude threshold (RMS > 2 nT/s), the influences of local time and season are largely removed, but the effects of the Swarm constellation prevail. Therefore, these plots are more suitable for evaluating the properties of the detected currents. Larger ratios of stable FACs are obtained in the afternoon sector, compared to the morning side, in particular in the northern hemisphere summer. For large structures, >150 km (>20s), we find ratios of almost 100% everywhere. This means, practically all magnetic variations can be regarded as caused by quasi-stationary FAC structures. Exceptions appear during November, December 2021. According to Figure 1 of Zhou et al. (2024), during those months the along-track separation between the satellites was above 20 s, increased up to 41 s on 16 December, after which it linearly decreased.

These ratio plots provide the opportunity to distinguish between the temporal and spatial correlation-lengths of the different FAC scales. From Figure 1 of Zhou et al. (2024) it can be seen that the along-track separation does not vary too much about its mean of ~5 s in the beginning of our study period up to mid-September. However, the longitudinal separation becomes progressively shorter. During these early months the occurrence ratios, for example of the 3-7 s and 7-13 s period structures exhibit at both hemispheres linear increases from the beginning of the study interval up to the date of coplanarity (1 October). We may attribute this behavior to the change of cross-track separation, and as expected, its influence is stronger the shorter the signal period. Quite differently, during the time after closest approach, here we find first a rapid decrease and after 16 December a recovery of the occurrence ratios. This variation of the ratio we like to attribute to the combination of growing along- and cross-track separations. It is worth noting that the ratios for all periods show approximately the same values at the beginning and end of the study time, when along- and cross-track separations have attained again similar values. For obtaining an estimate of the along-track separation on the ratio, one should first remove the cross-track effect, as observed during the time before coplanarity. Without going into details, it is obvious to see that also the along-track separation has a stronger effect on the shorter periods. The number of commonly observed stable structures, for example of 3-7 s period signals, is reduced by this effect to more than a factor of 2 at $\Delta t = 40$ s. Smaller reductions are derived for longer periods (larger scales). These observations provide a first idea of the FAC structure's temporal correlation lengths.

Somewhat special are the occurrence ratios obtained for the 1-3 s periods. Outside the true coplanarity period with $\Delta t = 2$ s the ratios are quite low, ranging between 10% and 20%. Interestingly, they do not approach zero. This indicates that there is another class of small (some 10 km) FACs that is stable over the range of along- and cross-track separations considered here. We will revisit this issue at the end of Section 5.2.

Another feature, worth to be noted, is the local minimum in FAC ratios on 4 November 2021. This coincides with the strongest magnetic storm during our study period. Suggested reasons for the reduced number of stable FACs are the more dynamic character of the currents with smaller scales and/or the expansion of the auroral oval beyond our limit of 60° MLat for the larger scales. No such effect on the ratios has been found during the other, weaker storm times. Interestingly, while the storm-related reduction of stable FACs is more prominent at shorter scales, there is a deeper dip in ratio at longest periods coinciding with the very quiet days on 27-29 October 2021.

An even more detailed view on the occurrence of selected FAC events is provided by Figure 6. It shows the latitudinal distribution of the ratio of stable FAC structures. The prime features of Figure 5 are also visible here, but this presentation offers another dimension. When starting with the first half of the study period, before the time of orbital coplanarity, we find for periods larger than ~20 s at all the latitudes, for all local times and both hemispheres high occurrence ratios. For shorter period, say <15 s, higher ratios tend to concentrate in the northern hemisphere at very polar latitudes. This could be due to some current properties, but it has to be taken into account that the orbital cross-over takes place close to the pole and with that, small cross-track separations are found there. However, when turning to the southern hemisphere (lower frame of Figure 6) we

https://doi.org/10.5194/angeo-2024-28
Preprint. Discussion started: 20 December 2024

conversely find, e.g. for the 7-13 s period band, largest ratios at the low-latitude end. This means, our expectation of large ratios near the cross-over is obviously not confirmed by the southern hemisphere observations. Rather, it seems that the season, summer in the norther hemisphere, is responsible for the preferred appearance of stable small-scale FACs at high latitudes. Conversely, in the southern, winter hemisphere these small-scale high-latitude FACs are missing, as is obvious from the blank parts in the plot near the pole. The effect of cross-track distance on this period band is stronger at lower latitudes. The larger distances, cause more reduced occurrence ratios in the morning and prenoon sectors than at afternoon to evening.

The second part of the study period exhibits more dynamic variations. Most prominent is the obvious drop in ratio during the time of extended along-track separation, Δt. As mentioned already above, the reduction is most pronounced for the small periods (short scales) and becomes less prominent the longer the period. On the upleg passes, covering the noon, afternoon sector, the reductions in ratio are quite evenly distributed over the latitudes. Conversely for the downleg, sampling night and early morning hours, there is a clear preference of ratio reduction at higher latitudes. Differently, the lower-latitude auroral FAC structures (e.g. R2 FACs) in this sector seem to be stable for more than 40 s.

Worth mentioning are also the two narrow features of low ratios around the beginning of November 2021. They represent contrasting activity conditions, the quietest period (27-29 October 2021) and the most intense storm on 3-4 November 2021 of the study period. In an attempt to explain the reasons for the low ratios we had a look at the cross-correlation plots from the two very different days. An example of a pass from the quiet day over the southern auroral region is shown in Figure 7, top frame. We find moderate activity in the morning and night sector at fairly high latitudes, around 70° MLat. For most parts of the orbital arc high correlation coefficients are obtained at the right time lag. Just the burst at night-time makes an exception. In spite of the primarily stable FAC structures on this quiet day, overall low ratios are obtained. This is caused by the relatively small amplitude of the signal, falling over large parts below our threshold of RMS > 2 nT/s. A quite different picture emerges from the stormy day on 4 November 2021. The example in the lower part of Figure 7 shows a northern hemisphere polar pass. Bursts of activity appear in the evening and morning sectors. Their amplitudes are an order of magnitude larger than those on the quiet day. The correlation coefficient generally stays below the threshold, $Cc = 0.75$, and also the optimal time lag is in most cases too short in comparison with the spacecraft separation. Another but minor effect is the equatorward expansion of the auroral activity during the storm to latitudes below 60° MLat and with that a movement out of our range activity monitoring. Large parts of the greatly expanded polar cap are practically free of signal. All this results in very few positive detections of stable FAC structures during this intense storm.

All the observations presented so far indicate that there are several processes that influence the stability of small- and meso-scale FAC structures. When looking at series of satellite observations, several of the controlling parameters vary at the same time. Therefore, it is not easy to disentangle the effects.

5. Discussion

The observations presented in the previous sections show that the correlation length of FAC structures have different dependences on spatial and temporal scales. In addition, also local time, season, latitude range and solar wind input may play a role. In this section we try to disentangle the various influences that determine the stability of a FAC structure. No effort has been undertaken so far to achieve this in comparable detail.

5.1 General characteristics of small- and meso-scale FACs

https://doi.org/10.5194/angeo-2024-28
Preprint. Discussion started: 20 December 2024

Annales Geophysicae Discussions

In a first step we look at the spatial scales and temporal lengths of stable FACs. Observations presented in Figure 5 indicate that the percentage of detected stable current structures depends on both the along- and cross-track separations between the Swarm satellites. For further investigating these dependences, Figure 8 presents the occurrence ratios for all the six band passes in d_{cross} versus Δt frames. The individual ratio percentages have been dropped into bins of 1 km for d_{cross} by 3 s for Δt. Bin averages are then shown in color. Results from both hemispheres are combined. Due to the given orbit geometry, the cross-over points are generally close to the geographic poles. Thus, only relatively small transverse separations are experienced in this high-latitude study. Within the range of d_{cross} = 0 - 15 km, as shown in Figure 8, we cover almost all the available cases (only a few reach up to d_{cross} = 20 km at Δt = 6 - 9 s). For classifying a current event as suitable for dual-SC FAC estimates we request occurrence ratios larger than 50%, as done in the earlier study by Zhou et al. (2024).

In general, Figure 8 confirms the impression gained from Figure 5, in particular for short period structures (small FACs); the occurrence ratios drop off rapidly away from the epoch of coplanarity. It is quite clear from Figure 6 that the patterns of occurrence ratios differ significantly between the upper and lower groups, the three shortest periods and the two longest, respectively, while the 13 - 23 s band contains something from both groups. Here we will go a little more into the details of the different characteristics observed for the two groups of FAC scale ranges.

The zonal correlation length of the meso-scale FACs (23-60 s) is obviously larger than the experienced satellite cross-track separations (0 -15 km). Therefore, the time between samples is more decisive for the occurrence ratio. Also here, larger structures are stable over a longer times. Generally, the 50% demarcation lines in Figure 8 lies for the lower two period bands beyond the covered Δt range. This confirms earlier studies, e.g. Gjerloev et al. (2011); Lühr et al. (2015), who reported stability periods of 60 s and more for FACs of these scale sizes. With the given limitations, the present study cannot provide much new information about the character of these meso-scale FACs at auroral latitudes. Still, it should be noticed, these results confirm well the applied preprocessing approach of the magnetic field recordings for the Swarm standard dual-SC FAC processing. For the calculations of those products the horizontal field components are low-pass filtered with a cutoff period of 20 s. This suppresses the variable small-scale signals. The along-track separation between Swarm A and C varies during normal operation between 4 and 10 s. In addition, there are the step sizes of 5 s, forming the integration quad (see Ritter et al. (2013) and Lühr et al. (2020) for more details). This means, measurements contributing to a dual-SC FAC density can be separated by up to 15 s. According to our results, the field recordings at the two spacecraft are still well correlated with each other. Figure 8 confirms that around 90% of the FAC structures with periods longer than 20 s are stable over even longer times than the 15 s.

The stability characteristics of structures with periods of 3 to 13 s are quite different. Their cross-track size seems to be the more limiting factor than the temporal stability. For example, in the case of the 3-7 s band, for small satellite separations, d_{cross} < 6 km, we find ratios of about 50% or more up to Δt ~ 16 s. Conversely, for larger cross-track separation, say d_{cross} > 8 km, we find nowhere 50% ratio levels for Δt > 4 s in this period band. Also in the 7-13 s bands, we find a similar tongue of elevated ratio levels for small spacecraft separations, d_{cross} < 6 km. This indicates that a majority of small-scale FACs exhibits such a narrow transverse sizes.

The FAC structures in the shortest period band seem to belong to another, third category of current features. Outside the Δt = 2 s separation range only very few common magnetic features are observed by the two Swarm satellites. These small FACs with horizontal scale of less than 10 km seem to be stable only for a second or so. Thus, the longitudinal separation of the spacecraft has no effect on the derived occurrence ratio. This type of small FAC is surely worth a more detailed investigation and may be the topic of a follow-up study.

https://doi.org/10.5194/angeo-2024-28
Preprint. Discussion started: 20 December 2024

Already Ishii et al. (1992) had reported about two types of FACs deduced from the ratio ΔB_{east} over E_{north}. The one, related to longer periods in satellite recordings, was identified as stable current structures. For such FACs it can be assumed that the field lines act as equal potential lines between magnetosphere and ionosphere. In those cases, the ΔB over $\mu_0 E$ ratio reflects the Pedersen conductance. These authors mentioned a short-period limit of 8 s for the stable FACs. Here we have identified a period around 15 s as the limit of stable meso-scale FACs. Although based on very different approaches, both studies come to consistent results for the typical scale range of stationary FACs. For shorter period (smaller) current structures Ishii et al. (1992) report a progressive increase of the E-field amplitude above that of ΔB down to transverse scales of a few kilometers. They call the FAC type observed here the transient Alfvénic mode. For even shorter scales the pure Alfvén mode is approached with $E/B = V_A$, where V_A is the Alfvén velocity. In the following we will focus on the FACs in the transient Alfvénic scale range.

5.2 Features of small-scale FACS

For learning more about the small FACs at auroral latitudes we looked into the distribution of stable events. Figure 9 shows in the upper two rows how the amplitude of the magnetic variations for selected FAC structures is distributed in magnetic latitude over our study period. The 3-7 s period band (~20-50 km wavelength) is used as example for this class of FACs. Only positive event detections within the above-described range, d_{cross} < 6 km and Δt < 18 s, are considered. Separate frames display the results from up- and downleg orbital arcs and from the two hemispheres. The blank areas, in particular at lower latitudes and times of large spacecraft separations, reflect the lack of entries due to our spatial/temporal constrains. Prominent stable current structures appear in the northern hemisphere near 80° MLat in the morning to noon sector during the first half of the study period. At the same time, much less activity is observed in the southern hemisphere with smaller amplitude and at somewhat lower latitude. We attribute this hemispheric differences primarily to the season, with local summer in the north and winter in the south. During night-time hours events appear at much lower latitudes and significantly smaller amplitudes. The second half of the study period is rather sparsely populated due to our constrains. Here we have southern summer conditions. As expected, more significant FAC activity appears in this hemisphere on upleg orbital arcs during morning and prenoon hours. Although we have winter in the northern hemisphere, it still shows appreciable small-scale FAC amplitudes in this time sector. The downleg arcs exhibit in the south some moderate FAC activity in the auroral region during pre-midnight hours. In the northern hemisphere the sampling is too sparse in this time interval for providing additional information.

In comparison to the identified stable small FACs, the two lower rows of Figure 9 shows the amplitude distribution of the deselected current events within the above-described range, d_{cross} < 6 km and Δt < 18 s in the same format. An obvious difference between the two distributions is the generally larger amplitude of the deselected events. This difference in amplitude is more pronounced on the nightside than on the dayside. On the nightside obviously only the really large FAC spike are unstable. The latitude distribution of deselected events is clearly narrower than that of the selected. This is in support of the preferred stability of the smaller amplitude FAC structures located away from the latitude of peak small-scale FAC activity. These facts suggests that the larger amplitude FACs tend to have smaller temporal and spatial correlation lengths. Here we should add a note. Not all the deselected events represent unstable current structures. In several cases one satellite may sample a stable FAC structure at the fringe while the other samples a different structure. That event will falsely appear under deselected. From the experience collected so far it probably concerns predominately the small-amplitude events that are falsely classified as deselected.

From the results presented in the upper rows of Figure 9 we suggest that the class of stable small-scale FACs detected in the range, d_{cross} < 6 km and Δt < 18 s, represent the majority of auroral zone FACs occurring in this size. In actual numbers, we detected about 230,000 stable FAC events in this very limited range, compared to a total of 340,000 stable events distributed over the whole spatial and temporal range. This fact provides additional evidence for the small correlation length of this type of FACs. Earlier studies of small-scale FACs, e.g. Kervalishvili and Lühr (2013), based on 5 years of CHAMP magnetic field data, found mean characteristics that resemble well this class in the 3-7s band. They report a clear preference of summer season for the noon-time amplitudes at cusp latitudes. A secondary activity peak appears in the night sector, which is less dependent on season, and lower activities show up on the dawn and dusk sides. Following the probability considerations, as outlined by Xiong and Lühr (2023) and Zhou et al. (2024), the mean correlation length of the current structure is expected to be twice as long as the spacecraft separation at the 50% occurrence ratio. In our case this means a distance of 12 km in azimuthal direction. From these results we may conclude that the common small-scale FACs at auroral latitudes are of filamentary character with short correlation lengths of the order of some 10 km.

Besides the above-described class of short-scale current structures there seems to be a minority of stable small-scale FACs exhibiting larger correlation lengths. In Figure 8 we find a horizontal band of slightly enhanced occurrence ratios (10%-20%) for d_{cross} = 12-15 km in the period band of 3-7 s. In this cross-track range the ratios vary only little with the along-track separation between the satellites. Such large cross-track distances are only experienced near the lower border, 60° MLat, of the considered latitude range. This second population of stable small-scale FACs is obviously a subauroral phenomenon, distinctly different from the first that prefers the cusp region and high latitudes. It would require additional investigations to characterize the features of this second population.

5.3 Characteristics of unstable small-scale FACs

From Figure 8 it is evident that even in the preferred small-scale FAC range, d_{cross} < 6 km and Δt < 18 s, of the 3-7 s period band detection ratios reach at best 60%. That means, about every second magnetic signature even in this favorable range is deselected. This is partly expected for a structure of finite size when one satellite passes close to the edge and the other samples another structure. There may, however, also be other reasons for deselection. For checking that we show in the lower two rows of Figure 9 the amplitude distribution of deselected events from the same spatial-temporal range as the selected above. When comparing the upper and lower pairs of rows, panel by panel, distributions are narrower in latitude for the deselected cases. The regions of deselected events are mainly populated by larger amplitude variations. Mean amplitudes of less than 4 nT/s are largely missing there. Thus, large-amplitude small-scale FACs are less stable than the smaller amplitude FACs, and this seems to be valid for both day and nightside events.

In the quest for reasons that favor unstable current structures we checked prevailing IMF and solar wind conditions during deselected events. As a parameter for representing the amount of solar wind input, we choose the merging electric field, E_m, as defined by Newell et al. (2007) (they call it coupling parameter)

$$E_m = \frac{1}{3000} V_{SW}^{\frac{4}{3}} (\sqrt{B_y^{\ 2} + B_z^{\ 2}})^{\frac{2}{3}} \sin^{\frac{8}{3}}(\frac{\theta}{2}) \tag{3}$$

https://doi.org/10.5194/angeo-2024-28
Preprint. Discussion started: 20 December 2024

where V_{SW} is the solar wind velocity in km/s, B_y and B_z, both in nT, are the IMF components in GSM coordinates, θ is the clock angle of the IMF. With these units the value of the merging electric field will result in mV/m. Here solar wind and IMF data, averaged over 1 min and propagated to the bow shock, are used to obtain a weighted time-integrated merging electric field which accounts for the memory effect of the magnetosphere-ionosphere system. Details of the approach can be found in the publication of Zhou et al. (2018).

For investigating the conditions accompanying our events we perform a superposed epoch analysis of the smoothed merging electric field. For the epoch of each event in the 3-7 s period band, occurring in the d_{cross} < 6 km and Δt < 18 s range, the E_m value evolution is considered from 30 min before the event to 30 min after it. The E_m time series from all the events are stacked and averages are calculated of each 1-minute bin. This provides the mean E_m, evolution around a certain class of small-scale FAC events.

Figure 10 shows the superposed epoch analysis results of the mean E_m evolution over the hour around the key time, $\delta T = 0$, for selected and deselected current structures as blue and red dotted lines, respectively. The two columns in Figure 10 represent results from the northern hemisphere on the left and from the southern on the right side. The curves in the top two panels are from the dayside, the ones in the two bottom panels are from the nightside. Seasonal effects may show up in a comparison between observations from days before and after 1 October 2021 (the epoch of coplanarity). Generally, we find larger E_m values accompanying deselected events than selected. Independent of season, hemisphere and local time, the level of E_m value ranges between 0.8 and 1 mV/m for the positively selected events. This represents well the mean merging electric field of quiet times during the considered months. Conversely, we obtain E_m > 1 mV/m for deselected events. Just during the months after 1 October 2021 E_m values below 1 mV/m are found in the northern hemisphere dayside for deselected events. This is cause by a generally low solar activity during the related days. Overall, the superposed epoch analysis confirms our earlier finding that large amplitude FAC structures are prone to instability, and the intensity of current density is largely dependent on the amount of solar wind driving. The evolution of the E_m values around the key time, $\delta T = 0$, does not provide a clear picture of the preconditions causing unstable FACs. The eight panels show various kinds of rising and falling trends of the red lines. Common to all is the elevated E_m value.

5.4 The roles of the deselection criteria

There is another question that we may address here. What kind of current variation causes the deselection of an event? The criteria for a stable current structure are, an amplitude RMS > 2 nT/s and a peak cross-correlation coefficient above 0.75 at a time lag agreeing with the along-track separation of the satellites within 1.5 s. By checking, which of the criteria causes the deselection, one may obtain information about the kind of variation. A general finding is that a low *C*c is involved in the large majority of deselected events. In the cases of a very low *C*c, it cannot be expected that the right T-lag is found. Therefore, a dropout of both criteria can also frequently be found. From this observation we infer that the large percentage of deselected small-scale events (up to period of 15 s) (see Fig. 8) is caused by a temporal or spatial change of the current signature between the visits by the two satellites.

In the case of meso-scale FACs high occurrence ratios, partly close to 100% (see Fig. 8), are observed. For large along-track separations the percentage drops somewhat. In order to find an explanation for that behavior we looked at the percentage of deselected events based solely on the T-lag criterion. Figure 11 shows the related ratio distribution in frames of d_{cross} over Δt, separately

https://doi.org/10.5194/angeo-2024-28
Preprint. Discussion started: 20 December 2024

Annales Geophysicae
Discussions

for the six period bands. The color scale represents the percentage of deselection by T-lag relative to the total number of deselected events. As mentioned before, the T-lag criterion plays hardly any role for the small-scale FACs. Corresponding ratios vary for periods up to ~15 s around 10%. We find a quite different picture for the meso-scale FACs, in particular for the longest period. The white gaps represent bins that contain no deselected events. This generally indicates the low count numbers of deselections on which these ratios are based. The fairly high percentage caused by T-lag, varying for the long periods, around 80%, indicates that a motion of the current system along the orbit track is the main cause here. This means, the FAC pattern does not vary in time, but the system is moving equator or pole ward. Such motions are well-know from auroral observations. The ratios for deselects by T-lag become progressively smaller for shorter periods, but the absolute number and distribution of these deselected events is quite similar over the period range 13 s - 60 s. That means, the latitudinal propagation of the current system is similar for the meso-scale FAC structures of different sizes. However, the change in dominant color from period to period indicates a clear reduction of stability, also for meso-scales, in space and time increasing towards smaller sizes.

6. Summary and Conclusions

In this study we made use of magnetic field data from the closely spaced Swarm A and C spacecraft during the counter rotating orbit phase. They allowed us to investigate the spatial and temporal correlation lengths of small-scale and meso-scale FAC structures at auroral latitudes. A number of detailed characteristics of small-scale FACs (10 - 70 km wavelength) have been identified for the first time. In particular, their stability features could be determined. Furthermore, the stationarity of meso-scale FACs (100 - 300 km wavelength) has been confirmed. The main findings of the study are:

1. The meso-scale FACs exhibit transverse (azimuthal) correlation lengths larger than our maximum spacecraft of 20 km. Therefore, no limit value can be provided here. Generally, large fractions of the current structures are identified as stable. Figure 5 shows for this class of FACs detection ratios close to 100% over most parts of the study period. Larger deflections from this level are confined to times of long along-track separations (up to 41 s) between the spacecraft. We identified the latitudinal motion of the current system as the main cause for the deselection of the events, not the temporal variation. All these results are consistent with earlier findings.
2. More interesting and new results have been obtained for the small-scale auroral FACs. For most of them an azimuthal correlation length of less than 15 km seems to be an important limit. A characteristic time period of less than 18 s has been obtained for their temporal stability. The distribution of current features identified in this limited spatial and temporal range agrees well with those of earlier studies about small-scale FACs. This includes their distribution in local time, magnetic latitude, and season. From these similarities we infer that our limits are typical for small-scale auroral FACs. However, during enhanced solar wind driving unstable small-scale FAC structures appear even in this limited spatial and temporal range.
3. An investigation of deselected small-scale current structures reveals that in particular the large-amplitude FACs are unstable. This is valid for the dayside and even more obvious on the nightside. In support of this fact, we could show that deselected events generally follow more intense solar wind driving. Stable current structures are accompanied by merging electric fields, E_m, with the value ranging between 0.8 and 1 mV/m, typical for low solar wind driving.
4. There exists another population of small-scale FACs that is stable over longer time, $\Delta t > 40$ s. Also, its azimuthal correlation width seems to be longer than 15 km. The preferred appearance

https://doi.org/10.5194/angeo-2024-28
Preprint. Discussion started: 20 December 2024

is at the equatorial end of our latitude range, near 60° MLat. No detailed investigations of these subauroral FACs have been performed, but they seem to be worth considering in a follow-up study.

From the results listed here we can conclude, the large-scale FACs are stable well over 40 s. Reasons for deselection are mainly the latitudinal motion of the current system, while its shape remains constant. Meso-scale FACs (100-300 km wavelength) also show the effect of latitudinal motion, but in addition, the shape starts to vary within 40 s. The smaller structures exhibit more variation. The small-scale auroral FACs exhibit quite different characteristics. They behave more like waves. Stable events are only found in a limited range of spacecraft separations both in time and spatial differences. Their stability is shorter than the Alfvén transition time from the magnetosphere to the ionosphere. The small-scale FACs with large amplitudes, e.g. during active periods (see Fig. 7 lower frame), have very short correlation lengths, falling below the resolution of this study. They seem to represent narrow solidary current structures that propagate along the field line in form of an Alfvén wave. Such intense narrow FACs can be found on the day and nightside. We may speculate that they are caused on the dayside by patchy reconnection and on the nightside by the bursty bulk flow. Multi-point measurements with higher spatial and temporal resolution would be needed to resolve the details of these intense solidary FACs.

Data Availability Statement

The authors thank the European Space Agency for openly providing the Swarm data. The data products used in this study are Level-1b MAGx_LR with version number 0602, which are available at the European Space Agency website: https://earth.esa.int/web/guest/swarm/data-access.

Author contributions

The study concept and the first draft of the manuscript were contributed by HL. Data collection and analysis were performed by YLZ. Both authors finalized the manuscript.

Competing interests

The corresponding author declares that none of the authors has a competing interests.

Acknowledgments

The work of Yun-Liang Zhou is supported by the National Nature Science Foundation of China (42174186).

https://doi.org/10.5194/angeo-2024-28
Preprint. Discussion started: 20 December 2024

Annales Geophysicae Discussions
Open Access

References

Anderson, B.J., H. Korth, C.L. Waters, D.L. Green, V.G. Merkin, R.J. Barnes, and L.P. Dyrud (2014), Development of large-scale Birkeland currents determined from the active magnetosphere and planetary electrodynamics experiment. Geophysical Research Letters 41: 3017–3025. https://doi.org/10.1002/2014GL059941.

Finlay, C. C., Kloss, C., Olsen, N., Hammer, M., Toeffner-Clausen, L., Grayver, A., & Kuvshinov, A. (2020). The CHAOS-7 geomagnetic field model and observed changes in the South Atlantic Anomaly. Earth Planets and Space, 72(1), 156. https://doi.org/10.1186/s40623-020-01252-9

Forsyth, C., I. J. Rae, I. R. Mann, and I. P. Pakhotin (2017), Identifying intervals of temporally invariant field-aligned currents from Swarm: Assessing the validity of single-spacecraft methods, J. Geophys. Res. Space Physics, 122, 3411–3419, doi:10.1002/2016JA023708

Friis-Christensen, E., H. Lühr D. Knudsen, and R. Haagmans (2008), Swarm-An Earth Observation Mission investigating Geospace, Adv. Space Res., 41(1), 210 – 216, doi:10.1016/j.asr.2006.10.008.

Gjerloev, J. W., S. Ohtani, T. Iijima, B. Anderson, J. Slavin, and G. Le (2011), Characteristics of the terrestrial field-aligned current system, Ann. Geophys., 29, 1713–1729.

Iijima, T. and Potemra, T. (1976), Field-aligned currents in the dayside cusp observed by Triad, J. Geophys. Res., 81, 5971–5979.

Ishii, M., M. Sugiura, T. Iyemori, and J. A. Slavin (1992), Correlation between magnetic and electric fields in the field-aligned current regions deduced from DE-2 observations, J. Geophys. Res., 97, 13,877–13,887.

Kervalishvili, G.N. and H. Lühr (2013), The relationship of thermospheric density anomaly with electron temperature, small-scale FAC, and ion up-flow in the cusp region, as observed by CHAMP and DMSP satellites, *Ann. Geophys., 32*, 541–554, doi:10.5194/angeo-31-541-2013.

Lotko, W., & Zhang, B. (2018). Alfvénic heating in the cusp ionosphere-thermosphere. Journal of Geophysical Research: Space Physics, 123, 10, 368–10,383. https://doi.org/10.1029/2018JA025990

Lühr, H., J. Park, J. W. Gjerloev, J. Rauberg, I. Michaelis, J. M. G. Merayo, and P. Brauer (2015), Field-aligned currents' scale analysis performed with the Swarm constellation, Geophys. Res. Lett., 42, doi:10.1002/2014GL062453.

Lühr, H., P. Ritter, G. Kervalishvili and J. Rauberg (2020), Applying the Dual-Spacecraft Approach to the Swarm Constellation for Deriving Radial Current Density, in *Ionospheric Multi-Spacecraft Analysis Tools*, M. W. Dunlop and H. Lühr (eds.), (ISSI Scientific Report Series; 17), 117-140, Springer Nature Switzerland.

Lysak, R.L. (1990), Electrodynamic coupling of the magnetosphere and ionosphere, Space Sci. Rev. 52, 33.

Neubert, T. and Christiansen, F. (2003), Small-scale, field-aligned currents at the top-side ionosphere, Geophys. Res. Lett., 30, 2010, doi: 10.1029/2003GL017808.

Newell, P. T., T. Sotirelis, K. Liou, C.-I. Meng, and F. J. Rich (2007), A nearly universal solar wind-magnetosphere coupling function inferred from 10 magnetospheric state variables, J. Geophys. Res., 112, A01206, doi: 10.1029/2006JA012015.

Ritter, P., H. Lühr, and J. Rauberg (2013), Determining field-aligned currents with the Swarm constellation mission, Earth Planets Space, 65(11), 1285–1294, doi:10.5047/eps.2013.09.006.

Rother, M., Schlegel, K., & Lühr, H. (2007). CHAMP observation of intense kilometre-scale field-aligned currents, evidence for an ionospheric Alfvén resonator. Annales Geophysicae, 25, 1603-1615. doi:10.5194/angeo-25-1603-2007.

Stasiewicz, K., et al. (2000), Small scale Alfvénic structure in the aurora, Space Sci. Rev., 92, 423–533, doi:10.1023/A:1005207202143.

Vogt, J. and Haerendel, G. (1998), Reflection and transmission of Alfvén waves at the auroral acceleration region, Geophys. Res. Lett., 25, 277–280, doi:10.1029/97GL53714.

Xiong C. & Lühr H. (2023). Field-aligned scale length of depleted structures associated with post-sunset equatorial plasma bubbles. *J. Space Weather Space Clim.* 13, 3. https://doi.org/10.1051/swsc/2023002

Zhou, Y.-L., Lühr, H., & Rauberg, J. (2024). Horizontal scales of small- and meso-scale field-aligned current structures at middle and low latitudes. Journal of Geophysical Research: Space Physics, 129, e2024JA032857. https://doi.org/10.1029/2024JA032857

Zhou, Y.-L., Lühr, H., Xu, H.-w., & Alken, P. (2018). Comprehensive analysis of the counter equatorial electrojet: Average properties as deduced from CHAMP observations. Journal of Geophysical Research: Space Physics, 123, 5159–5181. https://doi.org/10.1029/2018JA025526

https://doi.org/10.5194/angeo-2024-28
Preprint. Discussion started: 20 December 2024

Annales Geophysicae
Discussions
Open Access

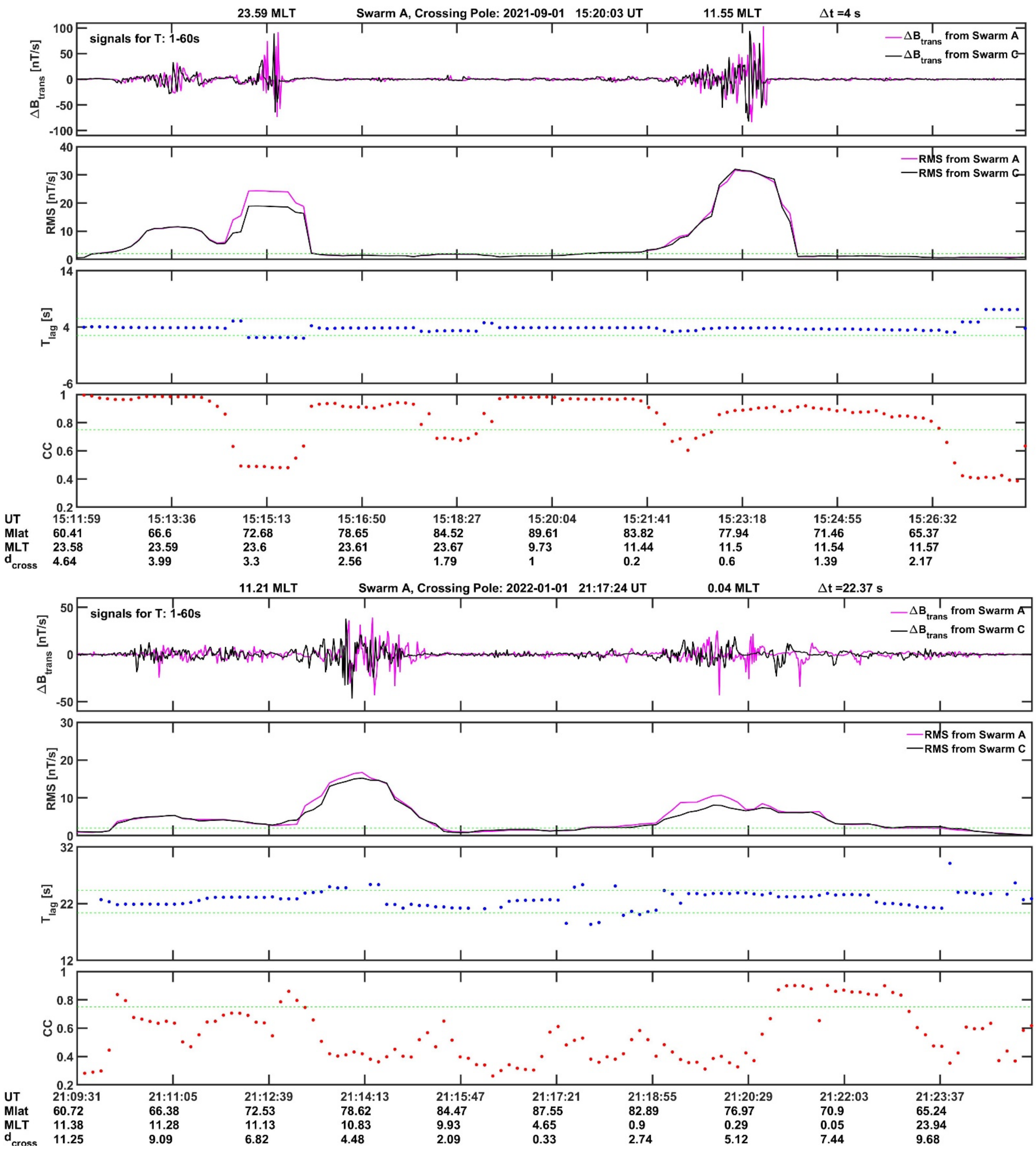

Figure 1. Examples of magnetic variations in the transverse, ΔB_{trans}, component within the period range of 1-60 s. The top panels of the two frames show the recordings of Swarm A and C along their orbits, crossing the polar region of the northern hemisphere. The second panel reflects the RMS value of the signal amplitude. The third panel contains the peak cross-correlation coefficient, *C*c. Significant correlations between Swarm A and C should have values, *C*c > 0.75. The dashed green lines mark the thresholds of the three detection criteria. The bottom panel shows the lag time, T-lag, between the signals at optimal correlation. T-lag values between the two green dashed lines indicate delays equal to the time separation between the spacecraft. The top frame is from a time with small along-track separation, Δt = 4 s and the bottom frame from a larger separation, Δt = 22.3 s

https://doi.org/10.5194/angeo-2024-28
Preprint. Discussion started: 20 December 2024

Annales Geophysicae
Discussions

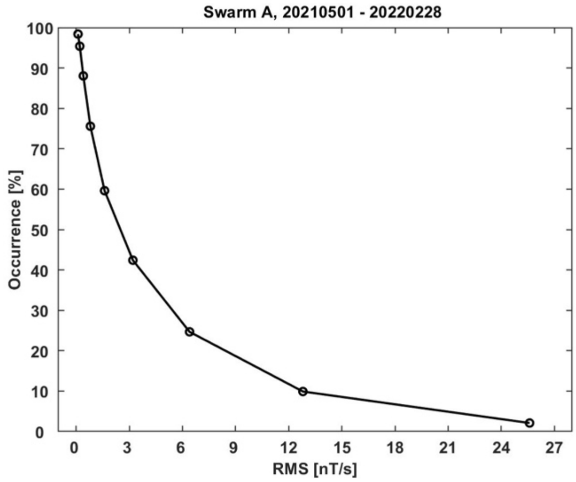

Figure 2. Occurrence distribution of transverse magnetic signature variations in the auroral region with amplitudes above a certain RMS value. Here, signals in the period range 1- 60 s (7.5 - 450 km along-track scale size) have been considered. For our FAC study amplitudes, RMS > 2 nT/s, are required. With that, about 50% of the signals are taken into account.

https://doi.org/10.5194/angeo-2024-28
Preprint. Discussion started: 20 December 2024

Annales Geophysicae
Discussions

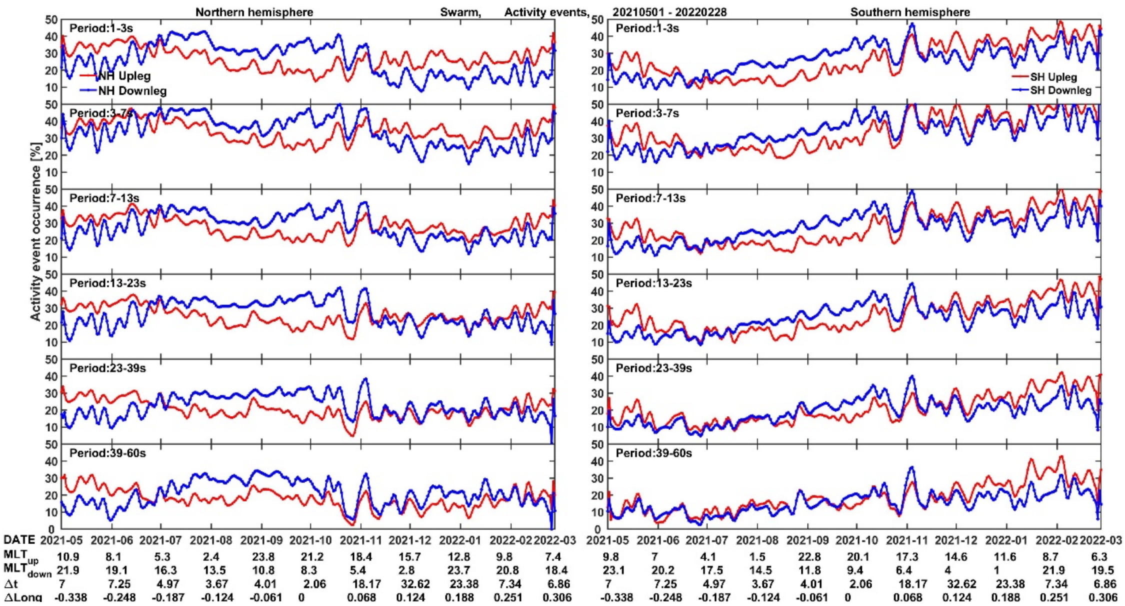

Figure 3. Temporal variation of all wave structures in the ΔB_{trans} component with amplitudes of RMS > 2 nT/s over the full study period, separately for the 6 period ranges and the two hemispheres. Results from the orbital upleg arcs at high latitudes (>60° MLat) are shown as red curves, those from downleg arcs are in blue. Across the bottom, besides the date, the local times at 70° MLat of the orbital arcs are listed, as well as the along-track time difference, Δt in seconds, between the spacecraft and the varying longitudinal separation at the equator, ΔLong, in degree.

https://doi.org/10.5194/angeo-2024-28
Preprint. Discussion started: 20 December 2024

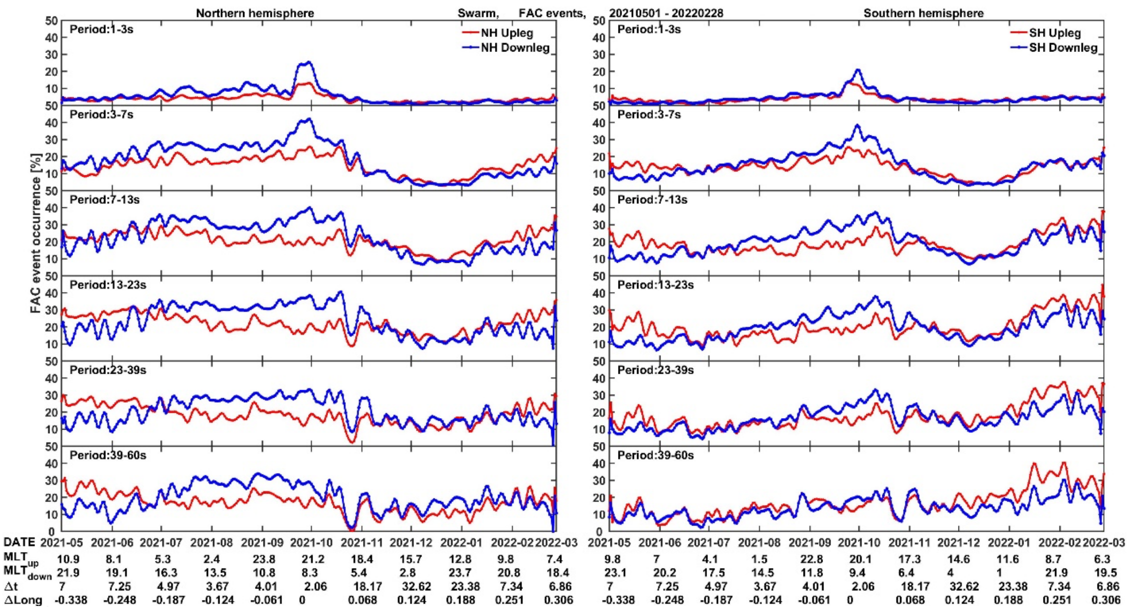

Figure 4. The same format as Figure 3, but for the occurrence frequency of positively detected static FAC structures.

https://doi.org/10.5194/angeo-2024-28
Preprint. Discussion started: 20 December 2024

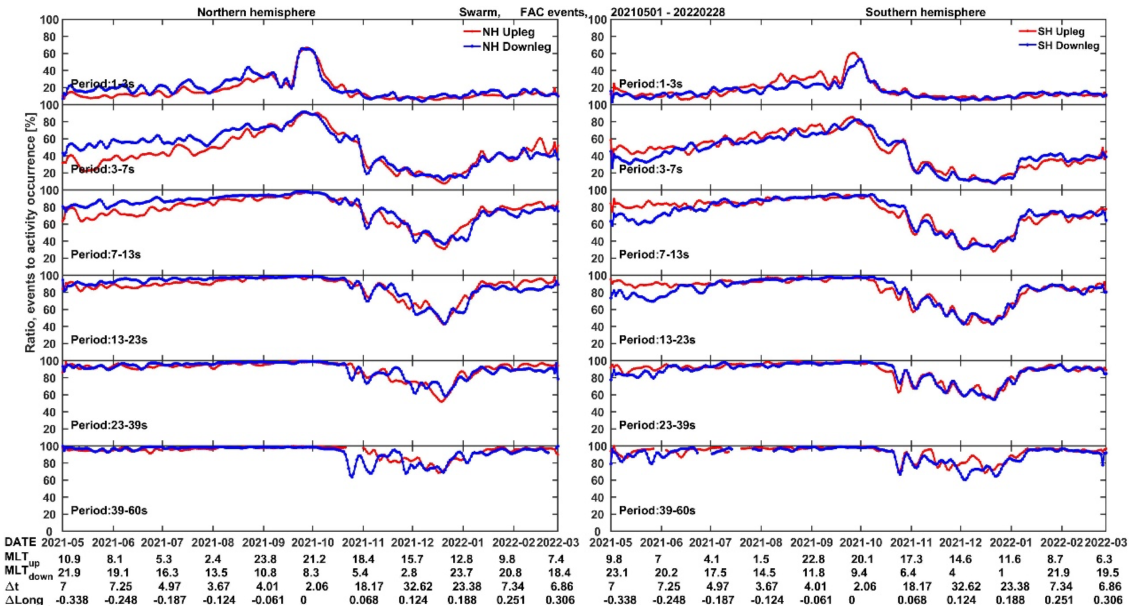

Figure 5. The same format as Figure 3, but for the ratio of detected static FAC structures (Fig. 4) divided by all the number of wave structures presented in Figure 3.

https://doi.org/10.5194/angeo-2024-28
Preprint. Discussion started: 20 December 2024

Annales Geophysicae Discussions

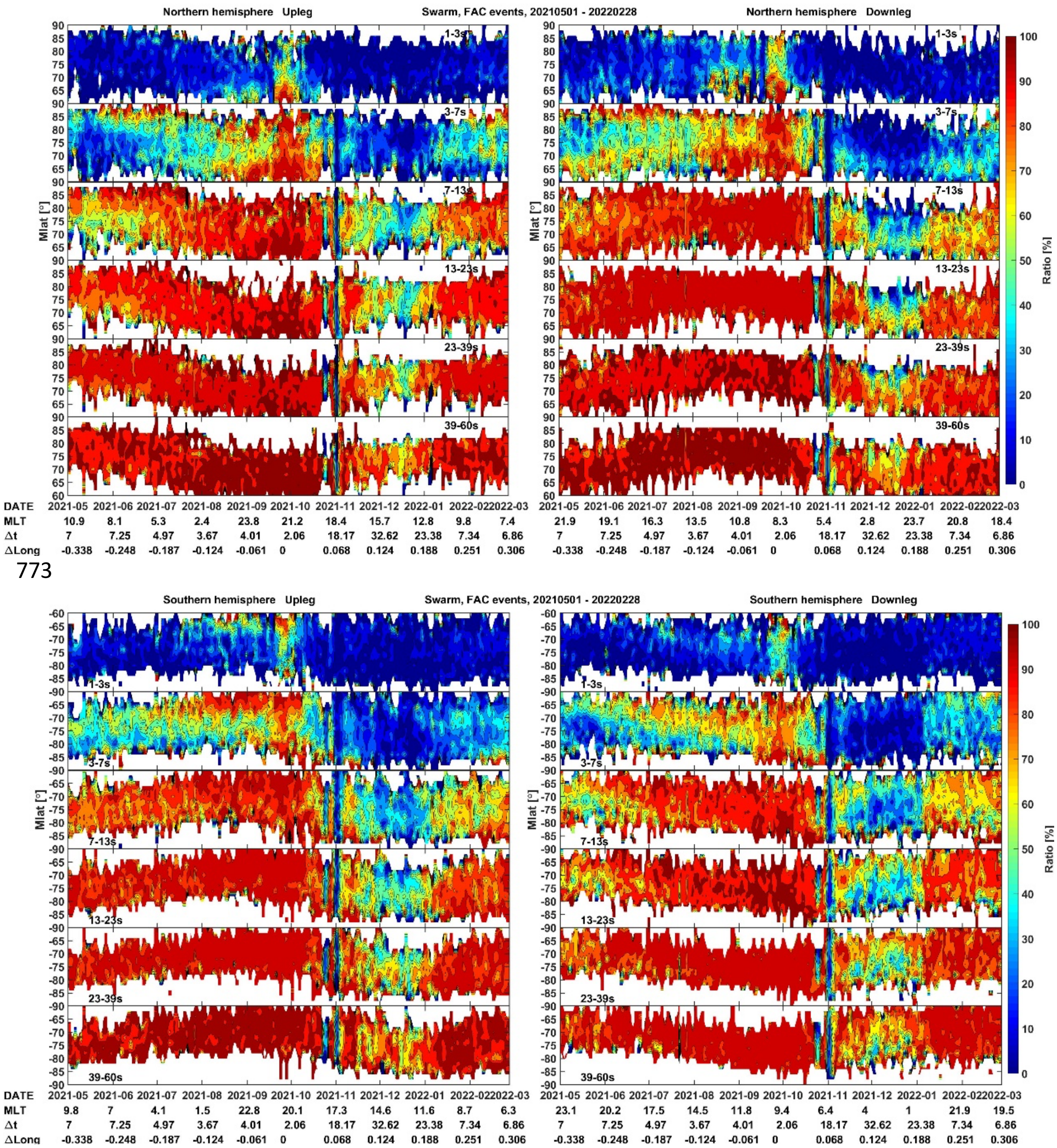

Figure 6. Latitude distribution of the ratio between positively detected static FAC structures and all wavy signals above the threshold of RMS > 2 nT/s, separately for all the six period bands, up- and downleg orbit arcs, and the two hemispheres. The labels along the horizontal axis are as described for Figure 3.

https://doi.org/10.5194/angeo-2024-28
Preprint. Discussion started: 20 December 2024

Annales Geophysicae
Discussions
Open Access

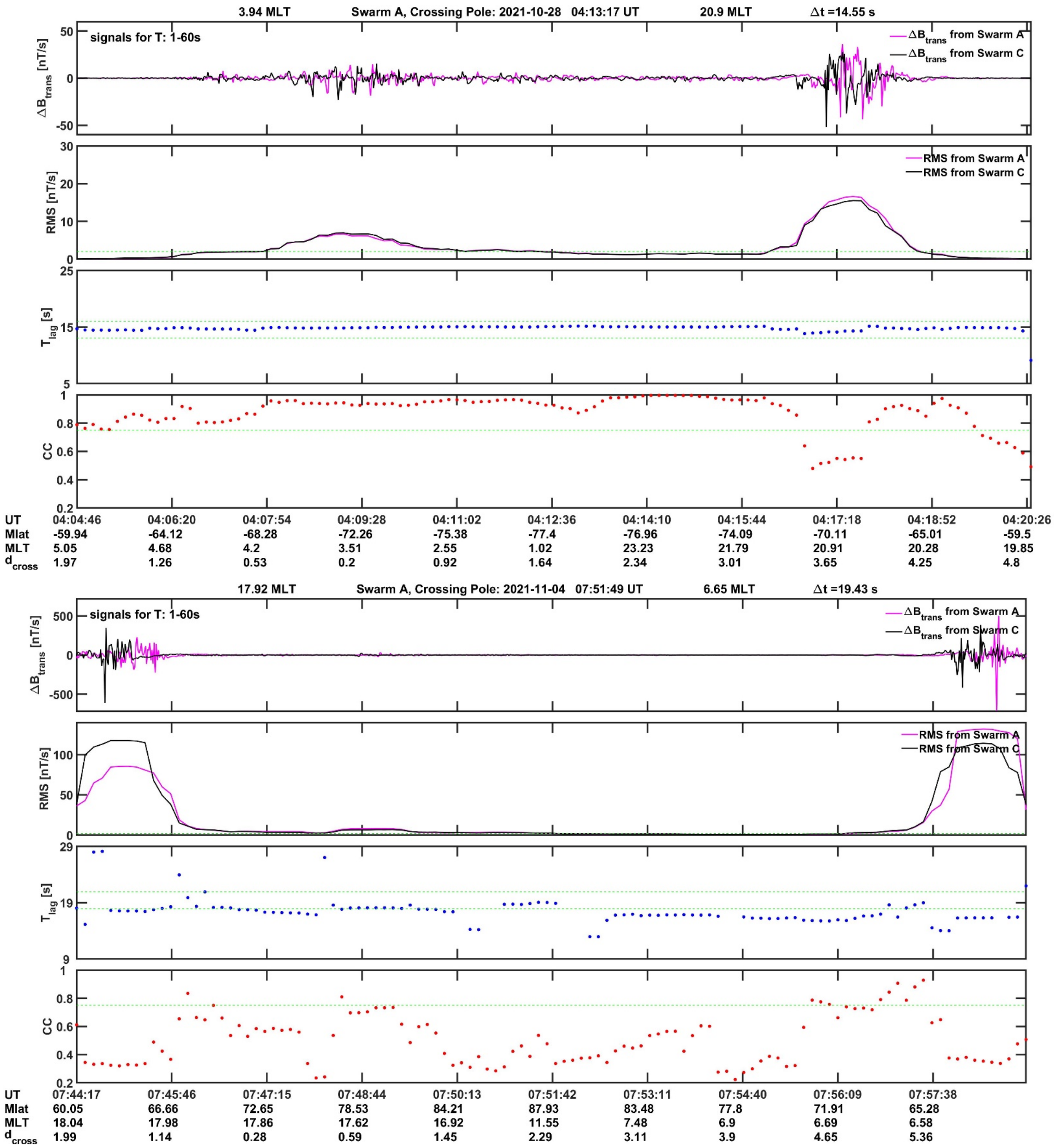

Figure 7. Magnetic variations in the transverse, ΔB_{trans}, components within the period range of 1-60 s in the same format as Figure 1. The top frame is from a very quiet day, while the bottom frame presents variations of the storm period on 4 November 2021. Peak amplitudes differ by a factor of 10 between the two days.

https://doi.org/10.5194/angeo-2024-28
Preprint. Discussion started: 20 December 2024

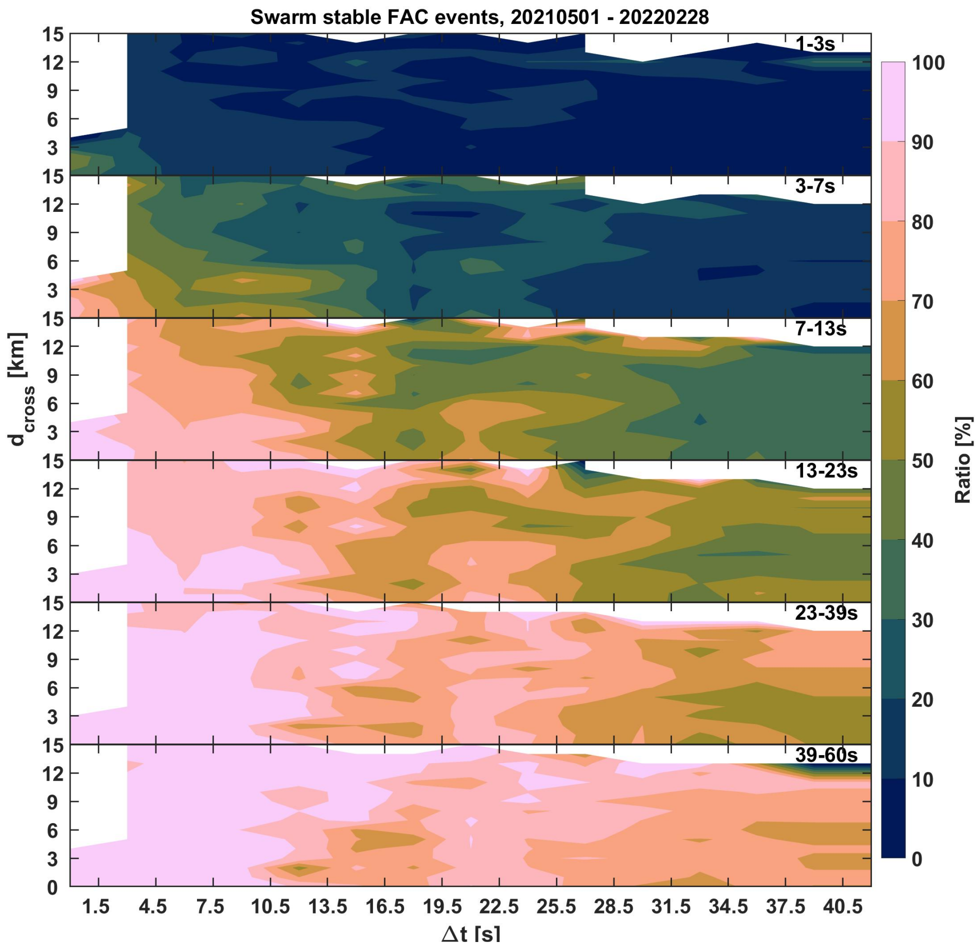

Figure 8. Distributions of stable FAC occurrence ratios in frames of cross-track distance, d_{cross}, versus along-track time separation, Δt, separately for the six period bands. There are hardly any measurements for d_{cross} > 15 km.

https://doi.org/10.5194/angeo-2024-28
Preprint. Discussion started: 20 December 2024

Annales Geophysicae
Discussions

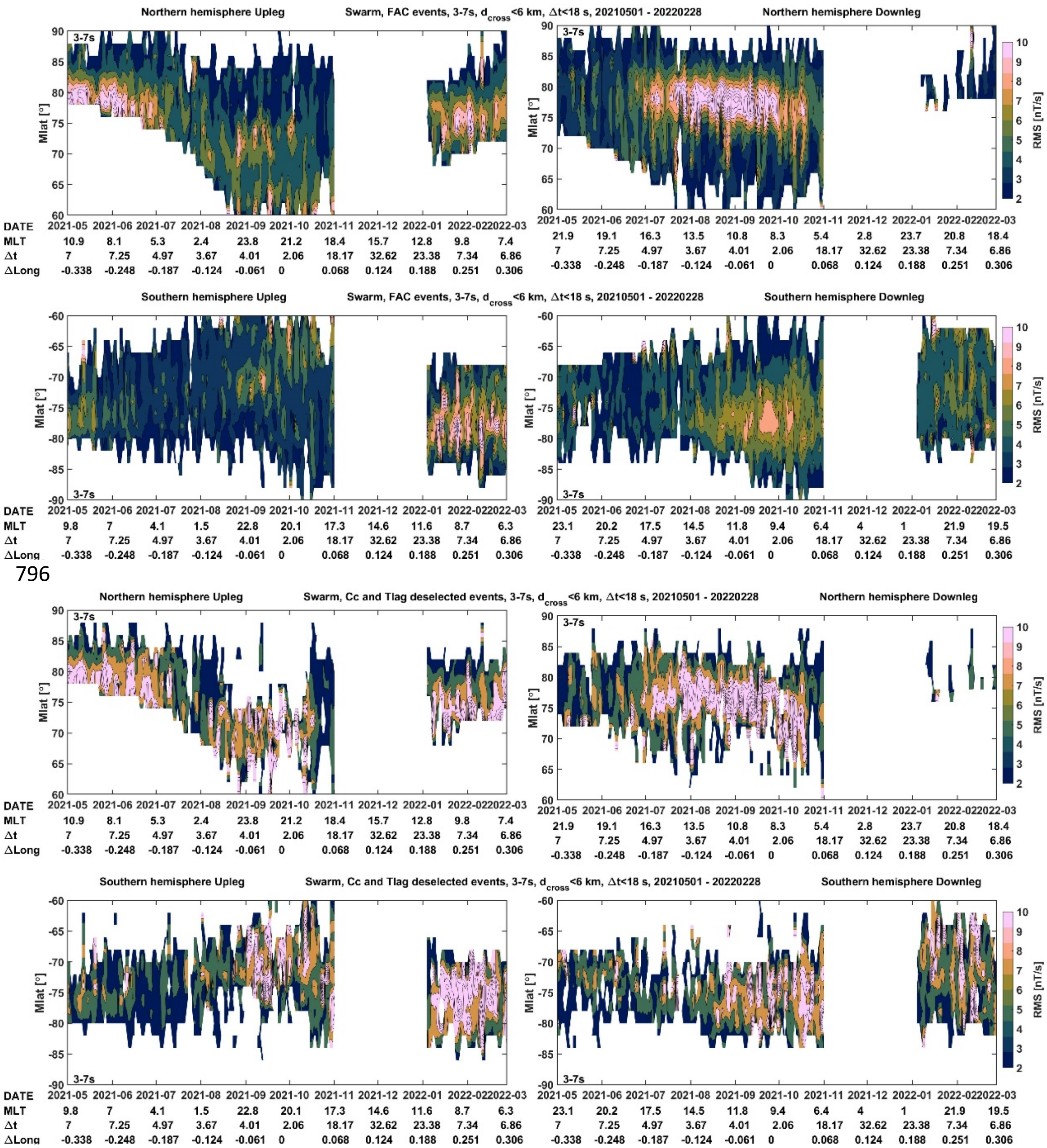

Figure 9. Amplitude distribution of small-scale magnetic variations over magnetic latitude. The format is the same as that of Figure 6, but only events from the 3-7 s period band and within the $d_{cross} < 6$ km and $\Delta t < 18$ s range are considered. The top two rows present the distribution of stable current structures and the bottom two row the deselected events. White areas mark ranges without entries.

https://doi.org/10.5194/angeo-2024-28
Preprint. Discussion started: 20 December 2024

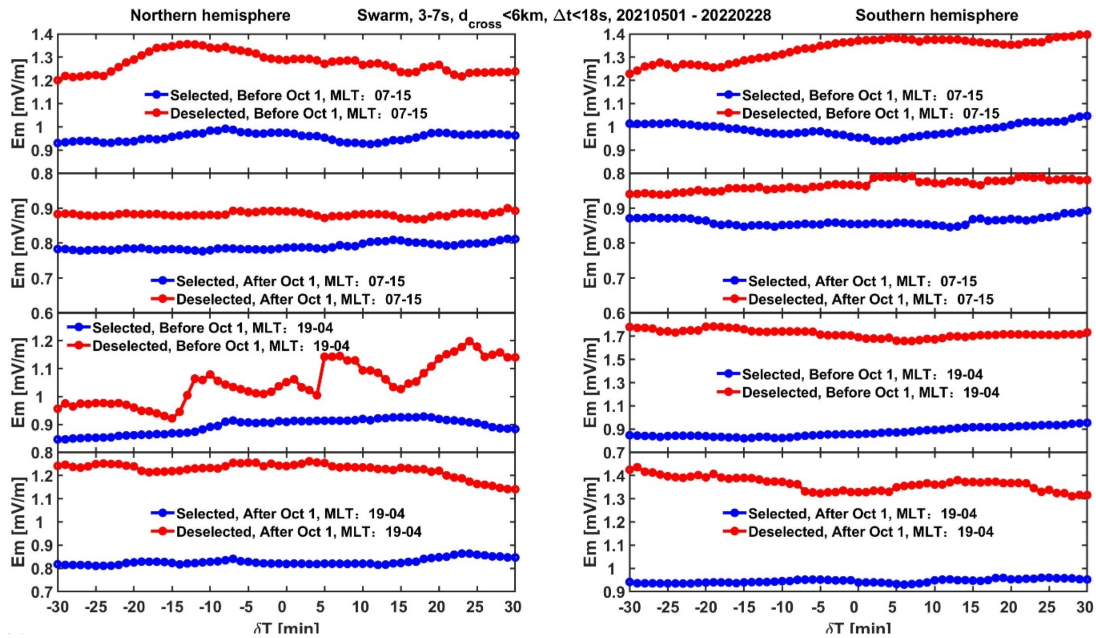

Figure 10. Superposed epoch analysis of the mean merging electric field, E_m, evolution accompanying the stable small-scale structures (blue lines) and deselected events (red lines). The relative time indicates the behavior before and after the FAC event detection. Individual analyses have been performed for dayside and nightside, for months around June and December solstices and for the auroral regions in the two hemispheres. The irregular curve of deselected events in the northern hemisphere after October is cause by the really small number of cases (see also Fig. 9).

https://doi.org/10.5194/angeo-2024-28
Preprint. Discussion started: 20 December 2024

Annales Geophysicae
Discussions

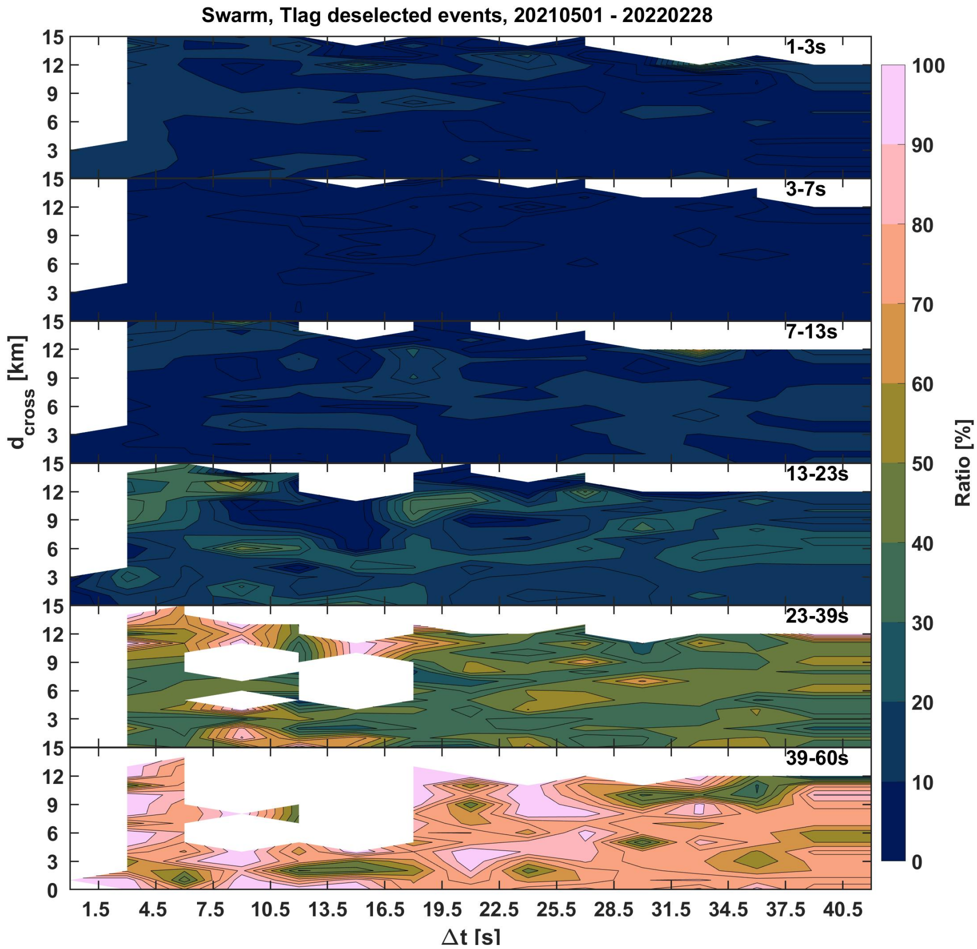

Figure 11. The same format as Figure 8, but for deselected events in the $d_{cross} < 6$ km and $\Delta t < 18$ s range based solely on the T-lag criterium. White patches represent bins without any deselected events. The T-lag criterium is of significance only for the meso- and large-scale FACs. Low cross-correlation coefficients clearly dominate the deselection of small-scale current structures.